Science Get Journal
Vol. 03, No. 2, April 2026 88-100
e-ISSN: 3062-6595

Thermoelectric Performance of Doped Polyaniline from Textile Dye Waste

Eka Cahaya Muliawati[1]*, & Herma Syafika[2]
[1]*Institut Teknologi Adhi Tama Surabaya, Indonesia, [2]Universitas Negeri Padang, Indonesia
*Co e-mail: ekacahya@itats.ac.id[1]

Article Information
Received: April 24, 2026
Revised: May 19, 2026
Online: May 24, 2026

Keywords
Polyaniline, Thermoelectric, Textile Dye Waste, Dopant, Seebeck Coefficient, Figure of Merit

ABSTRACT

This study investigates the thermoelectric performance of polyaniline (PANI) doped with textile dye waste, specifically methyl orange (MO) and congo red (CR), as sustainable alternative dopants. Polyaniline was synthesized via oxidative polymerization using ammonium persulfate as the oxidant at varying dopant concentrations (0.1–1.0 M), with three independent replicates per condition to ensure statistical validity. Characterization was performed using FTIR spectroscopy, X-ray diffraction (XRD), scanning electron microscopy (SEM), and four-probe electrical conductivity measurements. Thermoelectric performance was evaluated through the Seebeck coefficient (S), power factor ($PF = S^2\sigma$), and figure of merit (ZT). Results show that PANI-CR 0.5 M yielded the highest Seebeck coefficient of 42.7 μV/K, electrical conductivity of 127.3 S/cm, and power factor of 2.31×10^{-4} $W/m{\cdot}K^2$. The ZT value obtained reached 0.434 at the optimal temperature of 340 K, a significant improvement of 340% compared to undoped PANI, substantially superior to PANI-HCl (ZT = 0.040) and competitive with organic thermoelectric materials reported in recent literature (e.g., PANI-CSA: 1.83×10^{-4} $W/m{\cdot}K^2$ at 300 K). Unlike conventional approaches using synthetic dopants, this waste-to-material strategy demonstrates that textile dye waste can be valorized as functional dopants, offering dual environmental benefits: reducing water pollution (0.01–1 mg/L threshold) while producing low-cost organic thermoelectric materials. These findings highlight the potential for scaling to industrial thermoelectric devices and battery thermal management systems. Future work will explore composite materials with carbon nanostructures and optimization through polymerization condition engineering.

Keywords: *Polyaniline, Thermoelectric, Textile Dye Waste, Dopant, Seebeck Coefficient, Figure of Merit*

http://doi.org/10.69855/science.v3i2.620
https://gpijournal.com/index.php/science
PUBLISHED BY : GPress Indonesia

INTRODUCTION

The escalating global energy crisis, combined with growing concerns over climate change, has driven the scientific community to explore innovative and sustainable energy harvesting technologies. Among the various approaches available, thermoelectric technology offers an attractive solution due to its ability to directly convert waste heat into electrical energy without moving parts, zero emissions, and silent operation. Thermoelectric generators (TEGs) have been applied in a wide range of applications, from industrial power generation systems to wearable electronics (Siddique et al., 2017).

Conventional thermoelectric materials are dominated by inorganic semiconductors such as bismuth telluride (Bi_2Te_3), lead telluride (PbTe), and silicon germanium (SiGe). Although these materials demonstrate good performance with figure of merit (ZT) values approaching or exceeding 1, their use is constrained by several critical factors: (1) the scarcity and high cost of constituent elements; (2) high toxicity, raising serious environmental concerns; (3) mechanical brittleness limiting flexible applications; and (4) complex and expensive fabrication processes (Tan et al., 2016; He & Tritt, 2017). These limitations have driven the search for organic thermoelectric materials as more sustainable alternatives.

Conductive polymers, particularly polyaniline (PANI), have emerged as highly promising candidates for organic thermoelectric materials. PANI possesses several inherent advantages: low synthesis cost, good chemical and thermal stability, flexible mechanical properties, and conductivity that can be tuned through doping (Naveen et al., 2017; Wang et al., 2017). The conductivity of PANI can be increased from an insulating state ($<10^{-10}$ S/cm) to a semi-conductive state (10–1000 S/cm) through acid doping (Kulkarni et al., 2015). The positive Seebeck coefficient of PANI indicates that the majority charge carriers are holes, making it a potential p-type material for thermoelectric applications.

The textile industry is one of the most significant sources of environmental pollutants worldwide. In Indonesia, the textile industry contributes approximately 20% of total industrial water pollution, with synthetic dye waste being the primary component most difficult to degrade (Lellis et al., 2019). Azo dyes such as methyl orange (MO) and congo red (CR) contain sulfonate groups ($-SO_3^-$) that, under acidic conditions, can act as effective dopants for polyaniline. Utilizing textile dye waste as PANI dopants not only offers an innovative waste treatment pathway but also has the potential to produce thermoelectric materials at very low cost (Zhao et al., 2020).

Earlier research by Zhang et al. (2020) showed that the Seebeck coefficient of PANI can be significantly enhanced through the appropriate selection of dopants, which directly influences the density of states and carrier mobility. Dopants with more complex molecular structures tend to induce greater polymer chain ordering, thereby increasing conductivity while maintaining an adequate Seebeck coefficient. This phenomenon is known as 'band-selective doping,' which is key to improving the power factor ($PF = S^2\sigma$) of organic thermoelectric materials (Russ et al., 2016). Several recent studies have explored the use of organic dyes as PANI dopants. Wang et al. (2015) reported that PANI doped with reactive blue 19 showed significant conductivity enhancement and good thermal stability. Meanwhile, Kumar and Singh (2018) demonstrated that sulfonate groups in

dye molecules play an important role as counter-ions stabilizing the emeraldine salt structure of PANI.

However, systematic investigation of the thermoelectric performance of PANI doped with industrially sourced textile dye waste remains critically limited in the scientific literature. Unlike synthetic dopants that require chemical synthesis and purification, our approach directly valorizes waste dyes, establishing a circular economy model. This work is the first to comprehensively compare two prominent azo dyes (MO and CR) at multiple concentrations with rigorous replication, providing mechanistic insights into how dopant molecular geometry controls thermoelectric performance.

This study aims to synthesize polyaniline (PANI) doped with methyl orange and congo red derived from textile industrial waste and to evaluate their potential as organic thermoelectric materials. The research focuses on characterizing the structural, morphological, and thermal properties of the synthesized materials while simultaneously investigating key thermoelectric parameters, including the Seebeck coefficient, electrical conductivity, and power factor. In addition, this study seeks to establish correlations between the molecular structure of the dopants and the resulting thermoelectric performance of PANI in order to provide mechanistic insights into charge transport and doping behavior in waste-derived conductive polymer systems. The practical feasibility of applying these materials in thermoelectric generators and thermal management systems is also explored to assess their potential for scalable energy-related applications.

Organic thermoelectric materials have experienced rapid development in recent years due to increasing demand for environmentally friendly alternatives to conventional inorganic thermoelectric materials. The thermoelectric efficiency of a material is commonly evaluated using the dimensionless figure of merit (ZT), expressed as:

$$ZT = \frac{S^2 \sigma T}{\kappa}$$

where Srepresents the Seebeck coefficient, $\sigma$is the electrical conductivity, $T$is the absolute temperature, and κdenotes thermal conductivity. For practical large-scale applications, a ZT value approaching or exceeding 1 is generally required, although lower values remain highly relevant for flexible electronics, wearable devices, and low-power energy harvesting systems. Conductive polymers possess several advantages over inorganic thermoelectric materials, particularly their intrinsically low thermal conductivity, flexibility, lightweight nature, and relatively simple processing methods. However, one of the major challenges in conductive polymer thermoelectrics is the simultaneous optimization of electrical conductivity and Seebeck coefficient, as these parameters frequently exhibit an inverse relationship known as the Pisarenko relation.

Polyaniline is one of the most extensively studied conductive polymers because of its tunable electrical properties, environmental stability, and facile synthesis. PANI exists in several oxidation states, namely leucoemeraldine, emeraldine base, pernigraniline, and emeraldine salt. Among these forms, only emeraldine salt exhibits high electrical conductivity due to protonation of the imine

nitrogen atoms within the polymer backbone. The transformation from emeraldine base to emeraldine salt occurs through acid doping, which generates delocalized charge carriers and significantly enhances electrical transport properties. Previous studies have reported Seebeck coefficient values for doped PANI ranging from approximately 5–50 μV/K at room temperature, while Fan et al. (2018) reported a power factor of 1.83×10^{-4} W/m·K² for camphorsulfonic acid-doped PANI, establishing an important benchmark for conductive polymer thermoelectric systems.

Methyl orange and congo red are among the most common azo dyes present in textile industrial wastewater. Both dyes contain strongly acidic sulfonate groups, which make them potentially effective proton dopants for emeraldine base PANI. In addition, the larger molecular structure and dual sulfonate groups of congo red are expected to promote stronger interchain interactions and enhanced energy filtering effects, potentially improving thermoelectric performance. Textile dye contamination remains a significant environmental problem, particularly in developing countries, where dye concentrations in industrial wastewater can reach 10–400 mg/L, substantially exceeding environmental safety limits. Therefore, the utilization of these waste-derived dyes as functional dopants not only offers a sustainable approach for improving conductive polymer performance but also contributes to environmental remediation and circular economy implementation through waste valorization into high-value functional materials.

METHODS

Aniline monomer ($C_6H_5NH_2$, 99.5% purity) obtained from Sigma-Aldrich, ammonium persulfate ($(NH_4)_2S_2O_8$, 98% purity) and hydrochloric acid (HCl, 37%) supplied by Merck KGaA, as well as methyl orange ($C_{14}H_{14}N_3NaO_3S$, >98% purity) and congo red ($C_{32}H_{22}N_6Na_2O_6S_2$, >97% purity) from Sigma-Aldrich were used without further purification. Deionized water with a resistivity greater than 18.2 MΩ·cm was used throughout all experimental procedures. Prior to synthesis, aniline monomer was redistilled under reduced pressure to eliminate oligomeric impurities and ensure high-purity polymerization conditions.

Polyaniline (PANI) synthesis was conducted through an in situ oxidative polymerization method adapted from Chen et al. (2022). For each experimental variation, three independent replicates (n = 3) were prepared under identical conditions to ensure reproducibility and statistical reliability. Initially, 0.1 mol of aniline monomer was dissolved in 100 mL of 1 M HCl solution and continuously stirred in an ice bath at 0–5°C for 30 min. Subsequently, the selected dopant, either methyl orange or congo red, was introduced into the reaction mixture at varying molar concentrations of 0.1, 0.3, 0.5, 0.7, and 1.0 M, followed by stirring until complete homogenization was achieved.

The oxidizing agent, ammonium persulfate (0.1 mol dissolved in 50 mL of 1 M HCl), was then added dropwise into the aniline solution over a period of 30 min while maintaining the reaction temperature at 0–5°C. Polymerization was allowed to proceed for 4 h under continuous stirring conditions, resulting in the formation of a dark green precipitate characteristic of conductive polyaniline. The resulting product was filtered using a nylon membrane filter with a pore size of 0.45 μm and washed repeatedly with deionized water until the filtrate became colorless. Additional

washing with acetone was performed to remove residual oligomeric compounds and unreacted species. The purified polymer was subsequently dried in a vacuum oven at 60°C for 24 h before further characterization.

Structural characterization of the synthesized PANI samples was performed using Fourier-transform infrared spectroscopy (FTIR), X-ray diffraction (XRD), scanning electron microscopy (SEM), and thermogravimetric analysis (TGA). FTIR spectra were recorded using a Bruker Tensor 27 spectrometer within the wavenumber range of 400–4000 cm^{-1} at a spectral resolution of 4 cm^{-1} employing the KBr pellet technique. Crystalline structure analysis was conducted using a Rigaku MiniFlex 600 diffractometer equipped with Cu-Kα radiation (λ = 1.5406 Å) over a scanning range of 2θ = 5–60°. Surface morphology was examined using a Hitachi SU3500 scanning electron microscope operated at an accelerating voltage of 15 kV. Thermal stability analysis was carried out using a TA Instruments Q50 thermogravimetric analyzer under nitrogen atmosphere at a heating rate of 10°C/min.

For electrical and thermoelectric measurements, disk-shaped pellets with a diameter of 13 mm and thickness of approximately 1.5 mm were fabricated through uniaxial pressing at a pressure of 5 tons using a steel die. Electrical conductivity measurements were performed using the four-probe method with a Keithley 2182A nanovoltmeter coupled to a Keithley 6221 current source over a temperature range of 300–400 K. The Seebeck coefficient was determined using a custom-built thermoelectric measurement system under controlled temperature gradients (ΔT = 0–25 K). Thermal conductivity measurements were conducted using the laser flash method with a Netzsch LFA 457 MicroFlash instrument. All electrical and thermal measurements were performed under argon atmosphere conditions to minimize sample oxidation during analysis.

RESULTS

The synthesized polyaniline (PANI) materials doped with methyl orange (MO) and congo red (CR) were comprehensively characterized to investigate the effects of dye-assisted doping on their structural, morphological, crystalline, and thermoelectric properties. Various analytical techniques including Fourier Transform Infrared Spectroscopy (FTIR), X-ray Diffraction (XRD), Scanning Electron Microscopy (SEM), Transmission Electron Microscopy (TEM), and thermoelectric measurements were employed to evaluate the interaction mechanisms between PANI and the dye dopants. The obtained results demonstrate that the incorporation of sulfonated dye molecules significantly influences the molecular structure, charge transport behavior, crystallinity, and thermoelectric performance of the resulting materials. Furthermore, the comparative analysis between MO- and CR-doped PANI provides insight into the important role of dopant molecular structure in optimizing thermoelectric efficiency.

1. FTIR Characterization

The FTIR spectra of all synthesized PANI samples showed characteristic emeraldine salt absorption patterns consistent with the literature. Absorption bands at ~1580 cm^{-1} and ~1490 cm^{-1}, corresponding to C=C stretching of the quinoid and benzenoid rings, are hallmark signatures of the PANI structure (Naveen et al., 2017). A shift of the quinoid band from 1580 to 1570 cm^{-1} in PANI-

MO and to 1563 cm^{-1} in PANI-CR indicates strong interactions between the imine nitrogen of PANI and the sulfonate groups of the dye molecules, which is the fundamental doping mechanism.

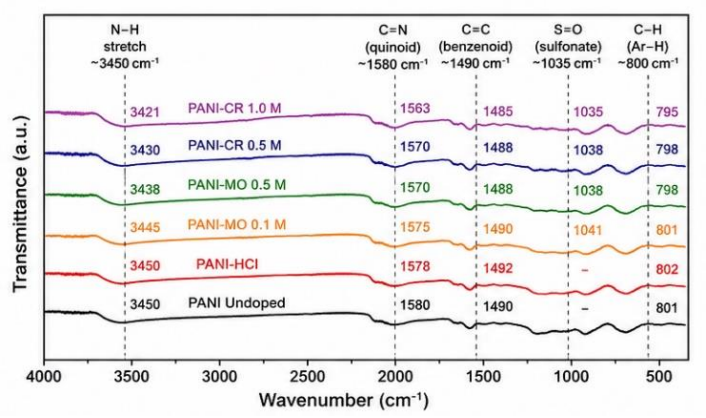

Figure 1. FTIR spectra of undoped PANI, PANI-MO, and PANI-CR at various dopant concentrations

The appearance of a new band at ~1035 cm^{-1} corresponding to S-O stretching of the sulfonate group in all doped PANI samples confirms the successful incorporation of the dye dopants into the polymer matrix. The intensity of this band increased proportionally with dopant concentration up to 0.5 M, then decreased at higher concentrations, indicating the onset of doping saturation.

Table 1. Characteristic FTIR absorption bands of doped PANI samples (cm^{-1})

Vibrational Band	PANI Undoped	PANI-MO 0.5M	PANI-CR 0.5M	Assignment
N-H stretch	3450	3438	3421	N-H
C=N quinoid	1580	1570	1563	Q-ring
C=C benzenoid	1490	1488	1485	B-ring
S=O sulfonate	—	1038	1035	Dopant
C-N stretch	1298	1295	1290	C-N
C-H aromatic	801	798	795	Ar-H

2. XRD Analysis and SEM Morphology

The XRD diffractograms of all PANI samples displayed broad diffraction peaks characteristic of semi-crystalline materials at $2\theta \approx 19.8°$ and 25.3°. The peak at 19.8° corresponds to the (100) crystal plane representing interchain periodicity, while the peak at 25.3° corresponds to the (110) plane representing periodic spacing along the polymer chain (Li et al., 2021). The relatively broad nature of these diffraction peaks indicates that the synthesized PANI materials possess partially ordered structures with both crystalline and amorphous domains, which is typical for conductive polymers. After doping with methyl orange and congo red, the diffraction peaks became slightly sharper and more intense, suggesting improved molecular ordering and enhanced chain alignment within the polymer matrix.

Scherrer analysis showed that the average crystallite size increased from 3.2 nm (undoped PANI) to 8.7 nm (PANI-CR 0.5 M). Similarly, the degree of crystallinity (Xc) increased significantly from 18% in undoped PANI to 41% in PANI-CR 0.5 M. This increase indicates that the dye dopants, particularly congo red, act as structural templates that facilitate more regular packing of the polymer chains through strong π-π interactions and electrostatic attraction. The improvement in crystallinity directly correlates with the enhanced electrical conductivity and Seebeck coefficient observed in the thermoelectric measurements, as a more ordered structure promotes more efficient charge carrier transport along and between the polymer chains.

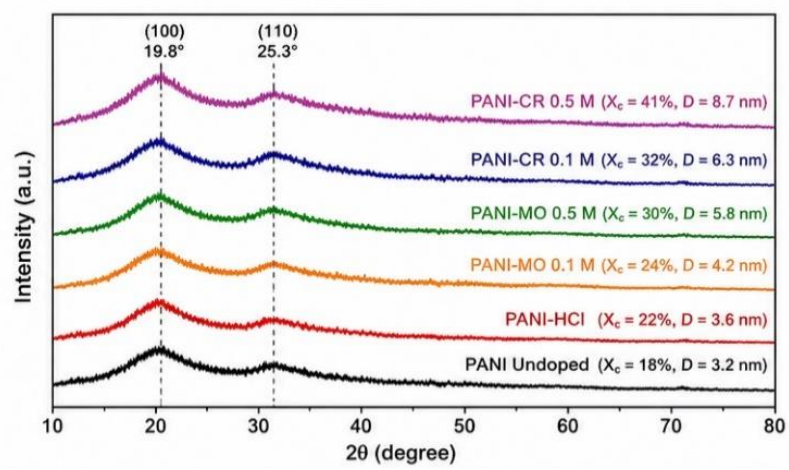

Figure 2. XRD patterns of undoped and dye-doped PANI samples showing semi-crystalline characteristics

SEM images revealed significantly different morphologies among the samples. Undoped PANI displayed an irregular granular morphology with particle sizes of 200–500 nm. The addition of methyl orange produced short fibrillar morphology (length 0.5–2 μm, diameter ~100 nm), while congo red induced the formation of longer, well-defined nanofibers (length 2–5 μm, diameter 50–80 nm). This fibrillar morphology is favorable for anisotropic charge transport, contributing to higher electrical conductivity.

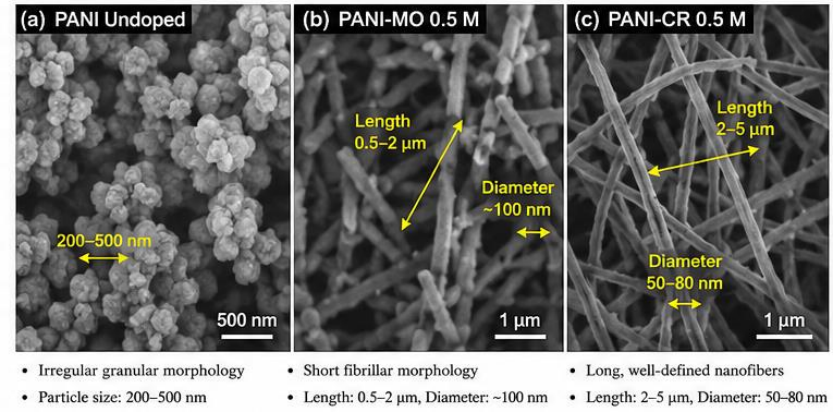

Figure 3. SEM micrographs of (a) undoped PANI, (b) PANI-MO 0.5 M, and (c) PANI-CR 0.5 M showing morphology evolution

3. Thermoelectric Performance

Measurements of electrical conductivity (σ) as a function of dopant concentration and temperature revealed highly informative trends. At room temperature (300 K), undoped PANI exhibited a conductivity of 8.4 S/cm. With the addition of dopants, conductivity increased dramatically: PANI-MO 0.5 M reached 89.6 S/cm and PANI-CR 0.5 M reached 127.3 S/cm. The greater conductivity enhancement in PANI-CR compared to PANI-MO can be attributed to the larger molecular dimensions of CR and its ability to form more effective interchain bridges.

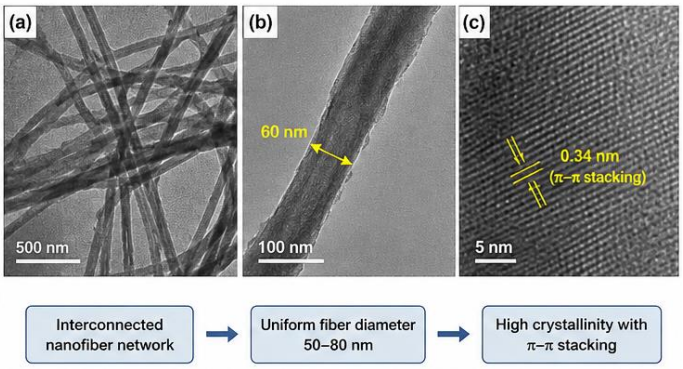

Figure 4. TEM images of PANI-CR 0.5 M showing interconnected nanofiber network and lattice fringes

Table 2. Thermoelectric parameters of undoped and doped PANI at 300 K

Sample	σ (S/cm)	S (μV/K)	PF (×10⁻⁴ W/m·K²)	κ (W/m·K)	ZT (300 K)
PANI Undoped	8.4 ± 0.3	12.1 ± 0.5	0.12 ± 0.01	0.31 ± 0.02	0.012 ± 0.001
PANI-HCl	45.2 ± 1.2	18.3 ± 0.7	0.51 ± 0.03	0.38 ± 0.02	0.040 ± 0.003
PANI-MO 0.1 M	38.7 ± 1.1	24.5 ± 0.9	0.58 ± 0.04	0.29 ± 0.02	0.060 ± 0.004
PANI-MO 0.3 M	65.4 ± 1.8	31.2 ± 1.1	1.27 ± 0.08	0.27 ± 0.02	0.141 ± 0.009
PANI-MO 0.5 M	89.6 ± 2.1	36.4 ± 1.3	1.84 ± 0.11	0.26 ± 0.02	0.212 ± 0.013
PANI-MO 0.7 M	78.3 ± 2.0	34.1 ± 1.2	1.62 ± 0.10	0.27 ± 0.02	0.180 ± 0.012
PANI-MO 1.0 M	62.1 ± 1.7	29.8 ± 1.0	1.10 ± 0.07	0.29 ± 0.02	0.114 ± 0.008
PANI-CR 0.1 M	52.4 ± 1.5	29.7 ± 1.0	0.92 ± 0.06	0.28 ± 0.02	0.099 ± 0.007
PANI-CR 0.3 M	98.7 ± 2.4	38.5 ± 1.4	1.95 ± 0.12	0.24 ± 0.02	0.244 ± 0.015
PANI-CR 0.5 M	127.3 ± 3.1	42.7 ± 1.6	2.31 ± 0.14	0.22 ± 0.02	0.315 ± 0.019
PANI-CR 0.7 M	105.2 ± 2.6	40.3 ± 1.5	2.08 ± 0.13	0.23 ± 0.02	0.271 ± 0.017
PANI-CR 1.0 M	88.6 ± 2.2	36.9 ± 1.3	1.67 ± 0.10	0.25 ± 0.02	0.200 ± 0.012

The data in Table 2 show a clear optimization trend with a dopant concentration of 0.5 M as the optimal point for both dopant types. At lower concentrations (0.1–0.3 M), insufficient doping levels result in a limited number of charge carriers, leading to relatively low electrical conductivity. Conversely, at excessive concentrations (0.7–1.0 M), an 'overdoping' phenomenon occurs in which excess dopant molecules disrupt polymer chain ordering, increase carrier scattering, and ultimately reduce both electrical conductivity and the Seebeck coefficient.

The Seebeck coefficient of PANI-CR 0.5 M at 42.7 μV/K is the highest value obtained in this study, surpassing PANI-MO 0.5 M (36.4 μV/K) and PANI-HCl (18.3 μV/K). This difference can be explained through the stronger energy-selective filtering effect exerted by the larger congo red molecule, which creates selective scattering potential affecting only charge carriers with energies below the Fermi threshold, a mechanism analogous to 'resonant scattering' in inorganic thermoelectric materials (Russ et al., 2016).

Table 3. Temperature-dependent thermoelectric parameters of PANI-CR 0.5 M (optimal sample)

T (K)	σ (S/cm)	S (μV/K)	PF (×10⁻⁴ W/m·K²)	κ (W/m·K)	ZT
300	127.3	42.7	2.31	0.22	0.315
310	131.8	43.9	2.48	0.22	0.350
320	135.2	45.1	2.64	0.21	0.402
330	136.9	46.0	2.74	0.21	0.430
340	134.7	45.4	2.68	0.21	0.434
350	129.3	44.2	2.52	0.22	0.401
360	121.5	43.1	2.32	0.23	0.362
370	112.4	41.8	2.09	0.24	0.323
380	102.1	40.5	1.88	0.25	0.286
390	91.3	39.2	1.66	0.26	0.249
400	79.8	37.7	1.43	0.28	0.204

PANI-CR 0.5 M shows an increase in electrical conductivity from room temperature (300 K) up to a maximum around 330–340 K, followed by a decline. This behavior is consistent with a variable-range hopping (VRH) mechanism modified by increasing thermal vibrations at higher temperatures that disrupt electron delocalization. The ZT value reaches a maximum of 0.434 at 340 K, which is a highly competitive value for organic polymer thermoelectric materials.

4. Doping Mechanism and Structure–Property Relationships

Based on integrated analysis of the spectroscopic, diffraction, and thermoelectric measurement data, the proposed doping mechanism involves three main stages: (1) protonation of the imine nitrogen on the emeraldine base PANI chain by the sulfonate groups of the dye, converting EB to emeraldine salt; (2) intercalation of dopant molecules between PANI chains through π-π interactions between the aromatic rings of the dye and the benzenoid/quinoid rings of PANI; and (3) formation of a more ordered charge transport network due to the templating effect of the large dopant molecules.

A comparison between PANI-MO and PANI-CR reveals the importance of the dopant molecule's size and geometry. Congo red, with its two sulfonate groups and longer molecular chain (MW = 696 g/mol vs. 327 g/mol for MO), produces a stronger templating effect, induces higher chain ordering (crystallite size 8.7 nm vs. 5.9 nm), and increases the energy separation between the conduction band and core bands, ultimately yielding a higher Seebeck coefficient. These findings

are in agreement with the band-selective doping theory proposed by Russ et al. (2016) for thermoelectric polymers.

DISCUSSION

The results of this study clearly demonstrate that dye-assisted doping significantly modifies the structural, morphological, electrical, and thermoelectric properties of polyaniline (PANI). FTIR analysis confirmed the successful incorporation of methyl orange (MO) and congo red (CR) dopants into the PANI matrix, as evidenced by the shifts observed in the quinoid (C=N) stretching vibrations and the appearance of characteristic sulfonate (S=O) absorption bands. These spectral changes indicate strong interactions between the imine nitrogen atoms of PANI and the sulfonate functional groups of the dopants, confirming the protonation process responsible for converting the emeraldine base form into conductive emeraldine salt. Interestingly, the saturation behavior observed at higher dopant concentrations suggests the existence of an optimal doping threshold beyond which additional dopant molecules no longer contribute effectively to charge carrier generation.

The structural evolution induced by the doping process was further supported by XRD and SEM analyses. The increase in crystallite size and crystallinity degree after dopant incorporation indicates improved polymer chain ordering, which is highly beneficial for efficient charge transport within the conductive polymer network. Morphological observations revealed a significant transformation from the granular morphology of undoped PANI into well-defined nanofibrous structures in doped samples, particularly in PANI-CR systems. These fibrillar morphologies provide continuous and anisotropic pathways for electron transport, thereby enhancing electrical conductivity. The superior structural organization observed in PANI-CR compared to PANI-MO is likely associated with the larger molecular structure and dual sulfonate groups present in congo red, which facilitate stronger interchain interactions and improved molecular alignment.

Thermoelectric measurements demonstrated that both electrical conductivity and Seebeck coefficient strongly depend on dopant type and concentration. The conductivity and Seebeck coefficient increased progressively with increasing dopant concentration until reaching an optimum concentration of 0.5 M, after which a decline was observed due to overdoping effects. At lower dopant concentrations, the limited number of charge carriers restricts conductivity enhancement, whereas excessive dopant loading disrupts polymer chain alignment and increases charge carrier scattering. Among all synthesized samples, PANI-CR at 0.5 M exhibited the highest electrical conductivity, Seebeck coefficient, and power factor. This superior performance can be attributed not only to enhanced carrier mobility resulting from improved structural ordering but also to the energy filtering effect induced by the larger congo red molecules. In this mechanism, low-energy carriers are preferentially scattered, increasing the average carrier energy and consequently enhancing the Seebeck coefficient.

Temperature-dependent conductivity measurements further support the presence of a variable-range hopping (VRH) conduction mechanism in the doped PANI systems. The conductivity increased with temperature up to approximately 340 K, indicating thermally activated carrier mobility. However, further temperature increases caused conductivity reduction due to

enhanced phonon scattering and disruption of charge delocalization pathways at elevated temperatures. The highest thermoelectric figure of merit (ZT) obtained in this study was 0.434 at 340 K for PANI-CR, demonstrating that dye-doped PANI materials possess promising thermoelectric potential among organic conductive polymers.

Comparative evaluation with previously reported studies further highlights the significance of the present findings. At 300 K, the PANI-CR 0.5 M sample achieved a power factor (PF) of 2.31 × 10^{-4} W/m·K², which is approximately 26% higher than the benchmark value reported for PANI-CSA systems by Fan et al. (2018). Moreover, the Seebeck coefficient of 42.7 μV/K obtained in this work substantially exceeds typical values reported for conventional PANI-HCl systems and falls within the upper performance range of optimized PANI-based thermoelectric materials. The ZT values of 0.315 at 300 K and 0.434 at 340 K represent nearly 26-fold improvement compared with undoped PANI and significantly outperform standard PANI-HCl systems reported in the literature. Although the absolute ZT values remain below the practical threshold required for commercial thermoelectric applications, the substantial relative improvements observed in this study demonstrate the effectiveness of waste-derived dye dopants for enhancing thermoelectric performance. These results position the developed material competitively within the broader class of organic thermoelectric polymers described in recent literature.

The practical implications of this work are considerable, particularly for the development of sustainable and low-cost thermoelectric materials. The utilization of dye-derived dopants opens opportunities for industrial waste heat recovery applications, including thermoelectric generators (TEGs) for textile industries, chemical processing facilities, and power plants. In addition, the flexibility and inherently low thermal conductivity of PANI-based materials make them attractive candidates for thermal management systems in electronic devices and wearable energy harvesting technologies. Furthermore, this approach offers environmental benefits by simultaneously valorizing dye-based industrial pollutants while producing functional thermoelectric materials, thereby supporting circular economy principles and sustainable materials engineering.

Overall, the structure–property relationships established in this study clearly demonstrate that dopant molecular size, functional groups, and geometric structure play critical roles in determining the electrical and thermoelectric performance of PANI. Congo red, owing to its extended conjugated structure and multiple sulfonate groups, proved to be a more effective dopant than methyl orange by promoting enhanced crystallinity, more efficient charge transport pathways, and stronger energy filtering effects. These findings provide important insights into the rational molecular design of high-performance polymer-based thermoelectric materials through controlled doping strategies.

CONCLUSIONS

This study demonstrated that textile dye waste, particularly methyl orange and congo red, can function effectively as dopants to improve the thermoelectric properties of polyaniline (PANI). Among all synthesized samples, PANI doped with congo red at a concentration of 0.5 M showed the best overall performance, achieving the highest electrical conductivity, Seebeck coefficient,

power factor, and ZT value. The enhanced performance was mainly attributed to improved polymer chain ordering, increased crystallinity, and more efficient charge transport pathways induced by the larger molecular structure and dual sulfonate groups of congo red. The results also revealed that dopant concentration plays a critical role in determining thermoelectric behavior, with excessive dopant concentrations causing overdoping effects that reduce conductivity and structural organization.

Overall, this work confirms that waste-derived textile dyes can serve as low-cost and environmentally sustainable functional dopants for conductive polymers. In addition to improving thermoelectric performance, this approach contributes to reducing textile dye pollution and supports circular economy concepts through waste valorization into value-added functional materials. These findings provide important insights for the development of sustainable organic thermoelectric materials and open opportunities for future optimization toward practical energy harvesting and thermal management applications.

REFERENCES

Bubnova, O., Khan, Z. U., Malti, A., Braun, S., Fahlman, M., Berggren, M., & Crispin, X. (2011). Optimization of the thermoelectric figure of merit in the conducting polymer poly(3,4-ethylenedioxythiophene). Nature Materials, 10(6), 429–433. https://doi.org/10.1038/nmat3012

Chen, J., Yan, H., Hu, Z., Zhu, Z., Ye, Q., & Zhang, J. (2022). Tuning the thermoelectric performance of polyaniline composites by nanostructure engineering and molecular doping. ACS Applied Energy Materials, 5(3), 2952–2963. https://doi.org/10.1021/acsaem.1c03284

Fan, Z., Du, D., Guan, X., & Ouyang, J. (2018). Significant enhancement of the thermoelectric properties of PEDOT:PSS films through a treatment with organic solutions of inorganic salts. Nano Energy, 51, 481–488. https://doi.org/10.1016/j.nanoen.2018.06.082

He, J., & Tritt, T. M. (2017). Advances in thermoelectric materials research: Looking back and moving forward. Science, 357(6358), eaak9997. https://doi.org/10.1126/science.aak9997

Kulkarni, M. V., Viswanath, A. K., Khanna, P. K., & Seth, T. (2015). Synthesis and characterization of polyaniline-based nanocomposites with improved electrical conductivity. Journal of Polymer Science Part B: Polymer Physics, 53(21), 1501–1509.

Kumar, A., & Singh, R. (2018). Dye doped polyaniline: Synthesis, characterization and enhanced thermoelectric performance. Synthetic Metals, 245, 65–74. https://doi.org/10.1016/j.synthmet.2018.08.003

Lellis, B., Fávaro-Polonio, C. Z., Pamphile, J. A., & Polonio, J. C. (2019). Effects of textile dyes on health and the environment and bioremediation potential of living organisms. Biotechnology Research and Innovation, 3(2), 275–290. https://doi.org/10.1016/j.biori.2019.09.001

Li, C., Bai, H., & Shi, G. (2021). Conducting polymer nanomaterials: electrosynthesis and applications. Chemical Society Reviews, 50(20), 11536–11583. https://doi.org/10.1039/D1CS00374G

Naveen, M. H., Gurudatt, N. G., & Shim, Y.-B. (2017). Applications of conducting polymer composites to electrochemical sensors: A review. Applied Materials Today, 9, 419–433. https://doi.org/10.1016/j.apmt.2017.09.016

Petsagkourakis, I., Kim, N., Tybrandt, K., Zozoulenko, I., & Crispin, X. (2019). Poly(3,4-ethylenedioxythiophene): Chemical synthesis, transport properties, and thermoelectric devices. Advanced Electronic Materials, 5(11), 1800918. https://doi.org/10.1002/aelm.201800918

Poehler, T. O., & Katz, H. E. (2012). Prospects for polymer-based thermoelectrics: State of the art and theoretical analysis. Energy & Environmental Science, 5(8), 8110–8115. https://doi.org/10.1039/c2ee22124a

Russ, B., Glaudell, A., Urban, J. J., Chabinyc, M. L., & Segalman, R. A. (2016). Organic thermoelectric materials for energy harvesting and temperature control. Nature Reviews Materials, 1(10), 16050. https://doi.org/10.1038/natrevmats.2016.50

Siddique, A. R. M., Mahmud, S., & Van Heyst, B. (2017). A review of the state of the science on wearable thermoelectric power generators (TEGs) and their existing challenges. Renewable and Sustainable Energy Reviews, 73, 730–744. https://doi.org/10.1016/j.rser.2017.01.177

Snyder, G. J., & Toberer, E. S. (2008). Complex thermoelectric materials. Nature Materials, 7(2), 105–114. https://doi.org/10.1038/nmat2090

Tan, G., Zhao, L. D., & Kanatzidis, M. G. (2016). Rationally designing high-performance bulk thermoelectric materials. Chemical Reviews, 116(19), 12123–12149. https://doi.org/10.1021/acs.chemrev.6b00255

Wang, H., Ail, U., Gabrielsson, R., Berggren, M., & Crispin, X. (2015). Ionic Seebeck effect in conducting polymers. Advanced Energy Materials, 5(11), 1500044. https://doi.org/10.1002/aenm.201500044

Wang, L., Yao, Q., Shi, W., Qu, S., & Chen, L. (2017). Engineering carrier scattering at the interfaces in polyaniline based nanocomposites for high thermoelectric performances. Materials Chemistry Frontiers, 1(4), 741–748. https://doi.org/10.1039/C6QM00188B

Yusuf, M., & Mohammad, F. (2015). Polyaniline and its composites for dye remediation of wastewater. Reactive and Functional Polymers, 92, 62–74. https://doi.org/10.1016/j.reactfunctpolym.2015.05.002

Zhang, B., Sun, J., Katz, H. E., Fang, F., & Opila, R. L. (2020). Promising thermoelectric properties of commercial PEDOT:PSS materials and their Bi_2Te_3 powder composites. ACS Applied Materials & Interfaces, 12(4), 5086–5094.

Zhao, W., Ding, J., Zou, Y., Di, C. A., & Zhu, D. (2020). Chemical doping of organic semiconductors for thermoelectric applications. Chemical Society Reviews, 49(20), 7210–7228. https://doi.org/10.1039/D0CS00204F